

# Assessment of groundwater vulnerability based on the modified DRASTIC model: A case study in Baicheng City, China

Mingjun Liu

Jilin University

Changlai Xiao

Jilin University

Xiujuan Liang (✉ [1916277955@qq.com](mailto:1916277955@qq.com))

Jilin University <https://orcid.org/0000-0003-4345-7791>

---

## Research Article

**Keywords:** Groundwater vulnerability, DRASTIC, Three-scale analytic hierarchy process, Weights of Evidence, Nitrate

**Posted Date:** May 14th, 2021

**DOI:** <https://doi.org/10.21203/rs.3.rs-460619/v1>

**License:**  This work is licensed under a Creative Commons Attribution 4.0 International License.

[Read Full License](#)

---

**Version of Record:** A version of this preprint was published at Environmental Earth Sciences on April 1st, 2022. See the published version at <https://doi.org/10.1007/s12665-022-10350-8>.



20 three-scale analytic hierarchy process (AHP) and the weights of evidence (WOE)  
21 methods were used to reassign the factor weights of the original DRASTIC model. The  
22 area under the receiver operating characteristic (ROC) curve, denoted as AUC, was  
23 used to quantitatively evaluate the accuracy of all five models (original DRASTIC  
24 model AUC: 0.62). By modifying the factors and weights, the four new models showed  
25 better performance, AUC values were 0.75, 0.76, 0.85, and 0.78 for the AHP-DRASTIC,  
26 AHP-DRASTICLE, WOE-DRASTIC, and WOE-DRASTICLE models, respectively.  
27 This indicates that the modified models could more accurately convey groundwater  
28 vulnerability in the study area. The WOE-DRASTIC model, which had the best  
29 performance, was then used to assess groundwater vulnerability in 2000 and 2010. In  
30 2000, 2010, and 2018, the proportion of areas with very high groundwater vulnerability  
31 increased from 5.14% to 6.34% to 7.93%, respectively. Meanwhile, the proportion of  
32 areas with very low vulnerability also increased, from 72.63% to 75.07% to 81.60%;  
33 demonstrating a situation of extremes. Findings of this study are expected to provide a  
34 new theoretical basis for the Baicheng municipal government in China to better manage  
35 and exploit groundwater resources.

36 **Keywords:** Groundwater vulnerability; DRASTIC; Three-scale analytic hierarchy  
37 process; Weights of Evidence; Nitrate

38

## 39 **1. Introduction**

40 Groundwater is an important drinking water resource because of its good seasonal  
41 storage capacity, stable temperature, nonsusceptibility to pollution, and convenience for  
42 exploitation. Baicheng City is an important commodity grain base in China, and  
43 groundwater is the main water source in most parts of the area, with 90% of water  
44 resources utilization from groundwater. In recent years, with the increase in population,  
45 the development of industry and agriculture as well as urban expansion have led to an  
46 increase in the extraction of groundwater, and further, the quality of groundwater has  
47 also deteriorated. Nitrate pollution is one of the main characteristics of groundwater  
48 pollution(Almasri, 2008; Jhariya, 2019), and is mainly caused by agricultural pesticides,  
49 chemical fertilizers, and industrial wastewater pollution. Polluted groundwater  
50 conditions are not easy to identify, and once present, such pollution is difficult to control  
51 and remediate. Therefore, to improve the sustainable development and utilization of  
52 groundwater, it is necessary to develop more effective prevention and control programs  
53 for groundwater pollution. Groundwater vulnerability assessment is the premise of such  
54 resource protection, facilitating rational development as well as better land use planning  
55 and groundwater resource management.

56 Three main methods for groundwater vulnerability assessment include: process-  
57 based simulation (Huan et al., 2016), statistical (Bonfanti et al., 2016), and index-  
58 overlay (Gogu & Dassargues, 2000; Huan et al., 2012). There is a wide global  
59 application of the index-overlay method; the representative models mainly include

60 DRASTIC, SINTACS, AVI, and GOD (Ferreira & Oliveira, 2004; Ghazavi & Ebrahimi,  
61 2015). The DRASTIC model (Aller et al., 1987) is the most widely used at present,  
62 owing to its ease of operation and ease of obtaining parameters. Moreover, its  
63 groundwater vulnerability assessment results can be presented in the form of a  
64 vulnerability map, which intuitively explains the distribution of groundwater  
65 vulnerability (Al-Adamat et al., 2003; Victorine Neh et al., 2015). However, in recent  
66 years, scholars have found the DRASTIC model to have certain deficiencies in the  
67 selection of model factors and weights. For example, the method fixes the weight and  
68 rates of each factor, without considering the actual real-world conditions, particularity  
69 of the study area (Rahim Barzegar et al., 2015; Brindha & Elango, 2015). Another  
70 limitation of DRASTIC is that it does not consider the effects of human activities on  
71 groundwater pollution. Therefore, it has become necessary to optimize the DRASTIC  
72 model such that more objective results can be achieved in combination with the actual  
73 conditions of the study area.

74 Theoretically, optimization of the DRASTIC model can be divided into two main  
75 aspects. First is the optimization of the assessment factors, which can be carried out by  
76 modifying the rating of factors, removing existing factors (An & Lu, 2018), or adding  
77 other parameters (Khosravi et al., 2018; Omotola et al., 2020). Gogu and Dassargues  
78 (2000), Babiker et al. (2005) and Wang and Yang (2008) have all suggested the addition  
79 of land use into the evaluation model because this factor is strongly related to  
80 groundwater vulnerability. Accordingly, Kazakis and Voudouris (2015) and Wu et al.

81 (2018) added land use factors to modify the model, and were able to improve the  
82 model's accuracy. At the same time, for this study, different degrees of groundwater  
83 over-exploitation are known to exist in certain parts of the study area, therefore this  
84 study adds not only land use (L)(Khan & Jhariya, 2019; Sener & Davraz, 2012) but also  
85 the degree of groundwater extraction (E) (Abu-Bakr, 2020) into the DRASTIC model  
86 to obtain the DRASTICLE model.

87 The second aspect is to optimize the weight of the parameters (R. Barzegar et al.,  
88 2018; Sahoo et al., 2016) . To do this, we refer to Pacheco et al. (2015), who adopted  
89 five methods to modify the weights of the DRASTIC model, and Khosravi et al. (2018)  
90 who applied four objective methods to modify the original DRASTIC model. Other  
91 modification strategies include the analytic hierarchy process (AHP)(Bai et al., 2012;  
92 Sener & Davraz, 2012; Thirumalaivasan et al., 2003), artificial neural network, fuzzy  
93 logic(Rezaei et al., 2013), logistic regression(Antonakos & Lambrakis, 2007) and the  
94 weights of evidence (WOE)(Khosravi et al., 2018) which are used to optimize the  
95 weights of parameters in DRASTIC models. In this study, two objective methods were  
96 used to modify the weights: the improved three-scale AHP and the WOE. The analytic  
97 hierarchy process (Saaty & Kearns, 1985) is simple to operate and has strong  
98 practicability and adaptability. The traditional AHP determines the judgment matrix  
99 using the nine-scale principle, yet with this method it is challenging to determine a  
100 reasonable judgment matrix because of the difficulty in grasping the importance degree  
101 among the parameters. Therefore, for this study, the three-scale method (Zuo, 1988)

102 was adopted to simplify the model, which is conducive for comparing the relative  
103 relations between parameters. In the improved three-scale AHP, the correlation between  
104 each parameter and nitrate concentration in the model was calculated and compared to  
105 determine the importance of the parameters, which overcomes the artificial subjectivity  
106 of the AHP and improves the accuracy of groundwater vulnerability assessment.  
107 Similarly, WOE is a geological statistical method that can solve the spatial analysis of  
108 multi-source information. The combination of the mature geographic information  
109 system platform and corresponding expansion module has not only been widely used  
110 in metallogenic prediction(Zhang et al., 2016), but has also been extended to other  
111 similar fields, particularly risk analyses such as landslide sensitivity analyses(Hong et  
112 al., 2017) and karst collapse risk zone division (Perrin et al., 2015). Barber et al. (1998)  
113 first applied WOE to regional groundwater vulnerability assessments with good results.  
114 Because of the high solubility and fluidity of nitrate, this compound easily transports to  
115 groundwater and is a good reflection of the degree of groundwater pollution (Shrestha  
116 et al., 2016; Voutchkova et al., 2021; Wang & Yang, 2008); thus, nitrate was selected as  
117 the response factor.

118 The main objective of this study was to use the DRASTIC model to evaluate  
119 groundwater vulnerability in the study area. First, the improved three-scale AHP and  
120 WOE were used to optimize the parameter weights of the DRASTIC model. Second,  
121 two additional parameters, land use and degree of groundwater extraction, were added  
122 to obtain the DRASTICLE model. To verify the accuracy and reliability of the model,

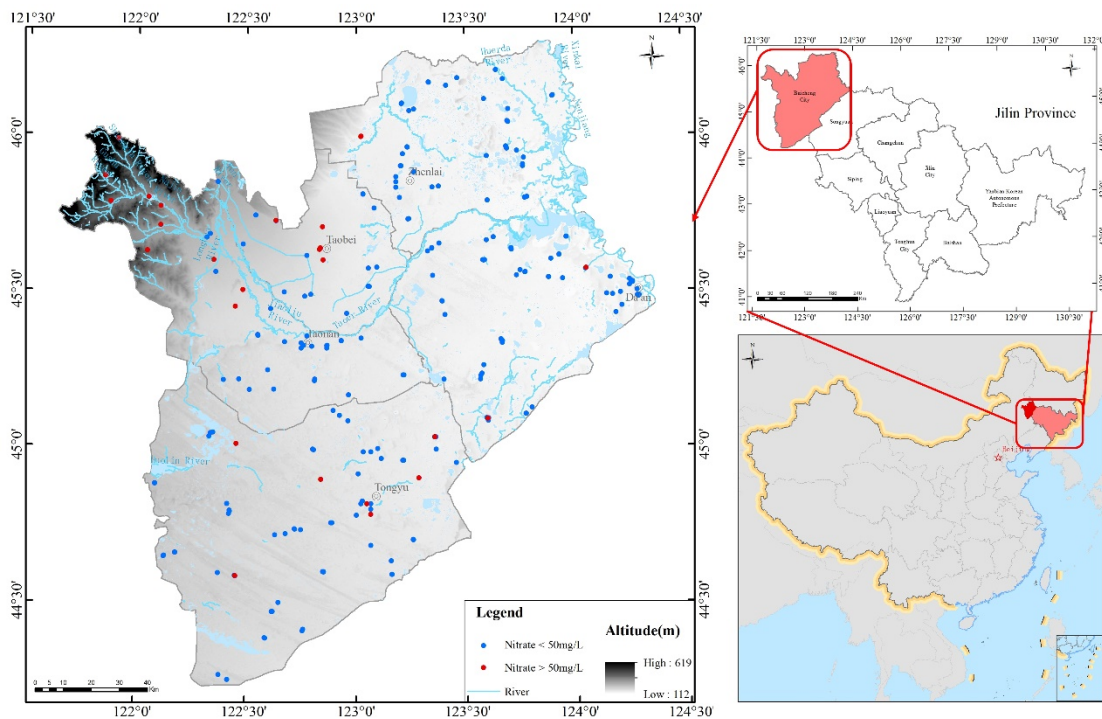
123 a receiver operating characteristic (ROC) curve was drawn based on the nitrate  
124 concentration, and the areas under the curve (AUC) of the DRASTIC, AHP-DRASTIC,  
125 AHP-DRASTICLE, WOE-DRASTIC, and WOE-DRASTICLE models were  
126 compared. The most effective model was identified and then used to evaluate the  
127 groundwater vulnerability of the study area in 2000 and 2010 and further analyze the  
128 associated temporal and spatial distribution of groundwater vulnerability.

## 129 **2. Study area**

130 Baicheng City is located in the northwestern part of Jilin Province, China, west of  
131 Songnen Plain, and east of the Horqin Grassland, and covers an area of approximately  
132 25600 km<sup>2</sup>, between longitude 121°38'06" to 124°23'56"E and latitude 44°13'57" to  
133 46°18'15.8"N (Fig. 1). The climate is a temperate continental monsoon with obvious  
134 seasonal changes. The average annual precipitation is approximately 400 mm, with an  
135 uneven distribution throughout the year. The average annual evaporation is 1340 mm,  
136 and the annual average temperature is 4.7°C. Low hills are situated in the northwest of  
137 the study area, with elevations of 300–662.6 m. The northeastern and southeastern  
138 plains are 130–140 m above sea level; in the southwest, a latent desert area is situated  
139 150–180 m above sea level. From the northwest to the southeast, the terrain of Baicheng  
140 comprises successive low mountains, hills, and plains, and is slightly uplifted in the  
141 southwest (Feng, 2019). The strata mainly include Carboniferous, Permian, Jurassic,  
142 Cretaceous, Neogene, and Quaternary.

143 In 2018, the Baicheng sub-center of the Jilin Water Environment Monitoring

144 Center performed sampling of 51 shallow groundwater monitoring wells in the city  
145 plain area during both April and September, which were tested for water quality  
146 parameters. The main items exceeding the standard were nitrate, ammonia nitrogen,  
147 manganese, fluoride, and arsenic. It shows that groundwater has suffered from different  
148 degrees of pollution. Associated land use types in the area are mainly cultivated land,  
149 accounting for approximately 60% of the study area, followed by grassland and saline-  
150 alkali land. From 2000 to 2018, the area of cultivated land and artificial surface both  
151 increased gradually, and the proportions of grassland and forest accordingly, gradually  
152 decreased.



153  
154 **Fig. 1** Location map of the study area and showing locations of sampling wells and nitrate  
155 distribution.

## 156 **3. Materials and methods**

### 157 **3.1 Source of data**

158 The meteorological data and hydrogeological data used in this study were  
159 collected and derived from the results of field measurements and sampling analysis by  
160 the project team. Data of groundwater depth, hydrochemistry, and groundwater  
161 exploitation were either provided by the Baicheng Water Resources Management  
162 Center or measured in the field by the project team. The groundwater depth data were  
163 collected from 1990 to 2018 at long-term monitoring wells, with each well dataset  
164 covering January–December, measured every five days, and the number of monitoring  
165 wells varied from 120–160 to per year. Nitrate data were collected from 202 wells in  
166 November 2017 by the project team and 52 wells were tested by the Baicheng Water  
167 Resources Management Center in April 2018. In addition, a total of 205  
168 hydrogeological boreholes were collected from this area.

169 Land use type data grids of Baicheng City in 2000, 2010, and 2018 with a  
170 resolution of  $30 \times 30$  m were downloaded from the National Catalogue Service for  
171 Geographic Information (<http://www.webmap.cn/main.do?method=index>) and  
172 GLOBELAND30 (<http://www.globallandcover.com/home.html?type=data>).

### 173 **3.2 DRASTIC model for groundwater vulnerability**

174 The DRASTIC model is mainly aimed at assessing the vulnerability of an  
175 unconfined aquifer. The model selects seven factors affecting groundwater flow and  
176 pollutant transport as vulnerability assessment parameters: depth to groundwater (D),  
177 net recharge (R), aquifer media (M), soil media (S), topography (T), impact of the

178 vadose zone (I), and conductivity of the aquifer (C). For this study, each parameter was  
179 classified according to its range of variation and internal attributes, and the  
180 corresponding vulnerability ratings were given; the larger the rating, the higher the  
181 vulnerability grade. The rating and weight of each factor for groundwater vulnerability  
182 have been previously described by Aller et al. (1987). The groundwater vulnerability  
183 index (VI) was calculated using Eq. 1:

$$VI = D_r D_w + R_r R_w + A_r A_w + S_r S_w + T_r T_w + I_r I_w + C_r C_w \quad (1)$$

184 where the subscripts r and w represent the ratings and weights for the seven  
185 parameters of the DRASTIC model, respectively.

186 Bojórquez-Tapia et al. (2009) indicated that five categories of groundwater  
187 vulnerability should be appropriate for conveying meaningful information to planners,  
188 decision-makers, and stakeholders. Therefore, in this study, the groundwater  
189 vulnerability index was divided into five categories: very low, low, moderate, high, and  
190 very high.

### 191 **3.3 Preparation of DRASTIC parameters**

192 Based on the original DRASTIC model, two factors affected by human activities,  
193 namely the type of land use (L) and degree of groundwater extraction (E), were added  
194 to generate the DRASTICLE model. All factors used in the model are described for this  
195 study as follows.

196 *Depth to groundwater (D)*. The depth to groundwater determines the contact time  
197 between the surface pollutants and aeration zone media before entering the aquifer.

198 Generally speaking, the greater the depth to groundwater, the greater the probability of  
199 pollutant attenuation and oxidation, and the lower the vulnerability of groundwater. The  
200 inverse distance weight tool of ArcGIS was used to process the groundwater table depth  
201 data of 120 long-observation wells in the research area, and the depth of the  
202 groundwater distribution map in the area was obtained. The groundwater depth was  
203 divided into five depth groups: 1.2–1.5, 1.5–4.6, 4.6–9.1, 9.1–15.2, and 15.2–17.3 m,  
204 and the corresponding ratings were given. The results are presented in Fig. 2a.

205 *Net recharge (R)*. Contaminants on the surface or soil can be transported vertically  
206 to groundwater through recharge water and transported within the aquifer. The greater  
207 the precipitation recharge, the greater the possibility of pollutants reaching the aquifer,  
208 that is, the greater the vulnerability trend of groundwater pollution. Many recharge  
209 sources of groundwater exist in the study area, including precipitation infiltration,  
210 lateral recharge in mountainous areas, river channel leakage, and well irrigation return  
211 recharge. The net recharge ranged from 51.2 to 236.8 mm and was divided into three  
212 categories, the results of which are shown in Fig. 2b.

213 *Aquifer media (A)*. The pore characteristics of the aquifer media determine the  
214 velocity of groundwater flow and affect the adsorption, diffusion, and dispersion of  
215 pollutants. In general, larger aquifer medium particles and more pores leads to the  
216 presence of better permeability, and lower probability of the pollutants being diluted  
217 and attenuated; thus, the higher the groundwater vulnerability. The object of this study  
218 was an unconfined aquifer, for which the fissure water aquifer was dominated by granite,

219 and the pore water aquifer was dominated by gravelly pebbles, loess sub-sand, and silty-  
220 fine sand. The Taoer River Fan phreatic aquifer is mainly composed of gravel and  
221 pebble gravel; sandy alluvial lacustrine plain is dominated by medium fine sand, fine  
222 sand, and silt, and the lithology of the swamp and saline-alkali valley is dominated by  
223 loess sandy soil (Fig. 2c).

224 *Soil media* (S). The soil medium affects the amount of surface water infiltrating  
225 underground, as well as the ability of pollutants to enter the aeration zone vertically.  
226 The surface of the study area is overlain by Upper Pleistocene and Holocene systems.  
227 The underlying Lower Pleistocene material is mainly distributed in the platform, which  
228 is a glacial moraine with a high clay content. The moraine deposits of the Upper  
229 Pleistocene Zhenxi Ice Age are mainly distributed in the fan and in the Taoer River and  
230 Jiao Liu River valleys. The upper ice-water accumulation layer is mainly composed of  
231 gravel, sand, and gravel with minimal clay, and is interbedded with clay, sub-clay, and  
232 fine sand lenses. The alluvium of the Guxiangtun Formation, which is mainly  
233 distributed in the alluvium plain, is a loess-like subsandy soil. Holocene alluvial  
234 deposits, which are distributed in the floodplain of the Taoer, Jiaoliu, and Hanhe rivers,  
235 as well as along the periphery of the fan front, are mainly composed of gravel, sand,  
236 gravel, and feature a subsandy soil layer. The associated aeolian sediments are  
237 comprised of yellow and white fine sand (Fig. 2d).

238 *Topography* (T). Slope mainly affects the infiltration of atmospheric precipitation.  
239 The lower the slope, the more infiltration is generated; thus, the higher the potential for

240 pollution. Slope distribution was extracted from digital elevation model data of  
241 Baicheng City using the ArcGIS surface analysis tool. The terrain in the study area is  
242 relatively gentle overall, though the hilly area in the northwest is relatively steep, with  
243 a topographic slope of up to 70%. The slopes in the area were categorized as 0–2%, 2–  
244 6%, 6–12%, 12–18%, and >18% (Fig. 2e).

245 *Impact of the vadose Zone (I).* The vadose zone controls the length of the  
246 infiltration path and seepage path of the surface water. The soil layer of the vadose zone  
247 has a remarkable ability to adsorb and block the entry of pollutants into groundwater.  
248 The better the sorting, the finer the particles and the higher the clay content of the  
249 vadose zone medium; thus, the worse the permeability, the stronger the adsorption and  
250 purification ability, the stronger the pollution prevention performance, and the weaker  
251 the groundwater vulnerability, hence the greater the vulnerability of the groundwater.  
252 The main lithologies in the vadose zone of the study area were found to be clay gravel,  
253 sub-sand, silty sand, loess sub-sand, sub-sand, gravel, gravel-bearing loess sub-sand,  
254 silt sub-clay, sand gravel, loess sub-clay, and gravel-bearing sub-sand. In the Taoer  
255 River Fan area, the lithology of the vadose zone was mainly gravel, while the valley  
256 area was sub-clay, and in the western low plain, the vadose zone was mainly silty sand  
257 and loess sub-sandy soil (Fig. 2f).

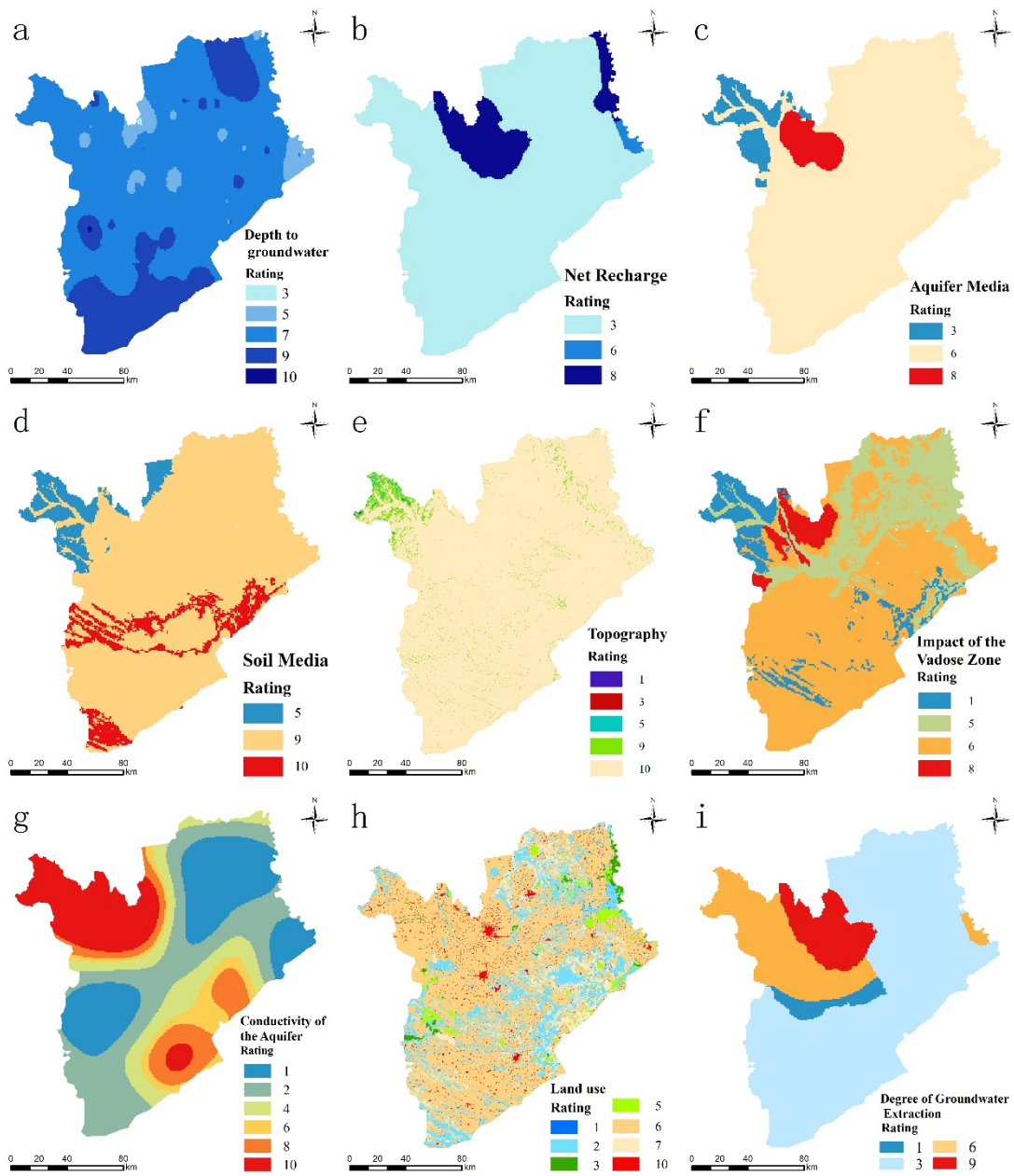
258 *Conductivity of the aquifer (C).* It controls the flow rate of groundwater and the  
259 migration rate of pollutants into aquifers. The conductivity of the aquifer varied  
260 significantly. Using the obtained permeability coefficient values of 157 wells, the

261 distribution of hydraulic conductivity in the area was obtained by simple kriging  
262 difference values, and the distribution pattern was roughly the same as the lithological  
263 distribution, ranging from 0.65–470.36 m/d. The Taoer River Fan had the largest  
264 hydraulic conductivity (Fig. 2g).

265 *Land use (L)*. The types and degree of pollution of pollutants produced by different  
266 land use types in the study area varied widely, while the surface cover can also be  
267 expected to have a great impact on the interception capacity of pollutants and the  
268 manner in which pollutants enter the aquifer. Typically, the vulnerability of  
269 groundwater in industrial areas is high, mainly because the distribution of factories is  
270 concentrated, and if the production wastewater is not discharged according to  
271 regulatory standards or is treated improperly and leakage occurs, the wastewater will  
272 likely become a potential source of groundwater pollution. In agricultural areas, wide-  
273 spread application of a variety of pesticides, fertilizers, and livestock and poultry  
274 manure can easily produce surface pollution sources, which pose a threat to  
275 groundwater quality. In green belt areas, such as grassland and forest, surface plants  
276 have the function of reducing surface runoff, reducing soil erosion, and adsorbing  
277 pollutants, thus such plants have a certain protective effect on groundwater, and the  
278 vulnerability of groundwater in these areas is lowest. The land use types in the study  
279 area were mainly divided into artificial surface, forest, water bodies, wetland, shrubland,  
280 cultivated land, grassland, and bare land (Fig. 2h).

281 *Degree of groundwater extraction (E)*. Groundwater exploitation intensity is

282 another major factor affecting groundwater vulnerability. Excessive exploitation of  
283 groundwater leads to an increased drop in groundwater levels and a larger scope of  
284 groundwater draw-down funnels, resulting in an increased hydraulic gradient.  
285 Meanwhile, as the formation of surface water and surrounding runoff stimulates  
286 groundwater recharge; groundwater becomes more vulnerable to pollution, which  
287 increases the vulnerability of the groundwater environment. The degree of groundwater  
288 extraction is the ratio of the actual extraction amount to the recoverable amount. The  
289 degree of groundwater extraction in Taobei District was 94%, the proportion of Taonan  
290 City in the Huolin River Basin was 14%, and most of the other areas were between 20%  
291 and 50% (Fig. 2i).



292

293

**Fig. 2** Maps of groundwater vulnerability conditioning factors: (a) depth to groundwater, (b) net

294

recharge, (c) aquifer media, (d) soil media, (e) topography, (f) impact of the vadose zone,(g)

295

conductivity of the aquifer, (h) land use, and (i) degree of groundwater extraction.

296

297

### 3.4 Factors correlation test

298

The evaluation factors in the model were expected to be relatively independent

299 and have no strong correlation; therefore, multi-collinearity diagnosis was performed  
 300 among the evaluation factors (Arabameri et al., 2019; O'Brien, 2007) to derive the  
 301 tolerance and variance inflation factor (VIF), with the thresholds of tolerance  $< 0.1$  and  
 302  $VIF > 10$  indicating strong multi-collinearity. The random point creation tool of ArcGIS  
 303 which was adopted to create 10000 random points in the research area, extract the rating  
 304 values of nine parameters corresponding to each point, and calculate the tolerance and  
 305 VIF using SPSS software.

### 306 **3.5 Optimization of DRASTIC model weights**

#### 307 **3.5.1 Three-scale analytic hierarchy process**

308 The three-scale AHP was used to modify the weights of the original DRASTIC  
 309 and DRASTICLE models, and has the same calculation steps as the traditional AHP.  
 310 The three-scale method was used to replace the original nine-scale method in order to  
 311 better construct the judgment matrix. The AHP was required to compare and judge  
 312 parameters and determine the order of their importance, the significance scale  
 313 comparison is presented in Table 1. In order to determine the magnitude relationship, a  
 314 correlation analysis between each parameter and the actual nitrate concentration was  
 315 carried out; the higher the correlation with nitrate, the more important the parameter. In  
 316 this way, the degree of importance of each parameter in the vulnerability assessment  
 317 could be determined.

318 **Table 1** Significance scale meaning table

---

Scale value	Description of two-factor relationship
-------------	--

---

---

0	The ci factor is less important than the cj factor
1	The ci factor is as important as the cj factor
2	The ci factor is more important than the cj factor

---

319

320 The VI of the AHP-DRASTIC and AHP-DRASTICLE models were calculated  
 321 according to Eqs. 1 and 2 , respectively.

$$322 \quad VI = D_r D_w + R_r R_w + A_r A_w + S_r S_w + T_r T_w + I_r I_w + C_r C_w + L_r L_w + E_r E_w \quad (2)$$

323 where the subscripts r and w represent ratings and weights for the nine parameters  
 324 of the DRASTICLE model, respectively.

### 325 **3.5.2 Weights of evidence**

326 Weights of evidence (WOE) (Agterberg & F., 1989) is a geostatistical quantitative  
 327 prediction method based on binary (existing or non-existent) images and Bayes' rule  
 328 under the assumption of independent conditions.

329 Assuming that the study area is A(T) km<sup>2</sup>, and the study area is divided into cells  
 330 of area U km<sup>2</sup>, the total number of cells in the study area is N(T)= A(T)/U. Assuming  
 331 that there are N(D) cells with response factor (D) distribution, the probability of the  
 332 occurrence of a response factor in any cell selected in the research area is P(D)= N(D)/  
 333 N(T), which is called the prior probability. It is assumed that the prior probabilities of  
 334 each cell are equal throughout the study area. Then, the prior probability is expressed  
 335 in terms of the odds (O):

$$O(D) = \frac{P(D)}{1 - P(D)} = \frac{N(D)}{N(T) - N(D)}. \quad (3)$$

336 The weights are calculated as follows:

$$W^+ = \ln \frac{P\{B|D\}}{P\{B|\bar{D}\}} = \ln \frac{N(B \cap D)/N(D)}{N(B \cap \bar{D})/N(\bar{D})}; \quad (4)$$

$$W^- = \ln \frac{P\{\bar{B}|D\}}{P\{\bar{B}|\bar{D}\}} = \ln \frac{N(\bar{B} \cap D)/N(D)}{N(\bar{B} \cap \bar{D})/N(\bar{D})}; \quad (5)$$

337 where B is the model factor, and D is the response factor (nitrate concentration).

338 The weight contrast is  $C = W^+ - W^-$ , and the standard deviation of the weight

339 difference is  $\sigma = \sqrt{\sigma^2(W^+) + \sigma^2(W^-)}$ , where  $\sigma^2(W^+)$  and  $\sigma^2(W^-)$  are the

340 variances of  $W^+$  and  $W^-$ , respectively. The final weight is  $W = \frac{C}{\sigma(C)}$ .

341 The WOE requires that the distribution of predictors relative to the response factor

342 satisfy condition independence. For n predictors, if all are conditionally independent

343 with respect to the response factor, the logarithm of the odds is:

$$\ln R = \ln \left\{ O \left[ \frac{D}{B_1^k B_2^k \dots B_n^k} \right] \right\} = \sum_{j=1}^n W_j^k + \ln O(D); \quad (6)$$

$$(j = 1, 2, 3 \dots, n).$$

344 Finally, by using the formula  $P = \frac{R}{1+R}$ , the logarithm of the posterior odds can be

345 transformed into posterior probability.

### 346 **3.6 Comparison and validation of models**

347 To validate and compare the accuracy of the five models, the ROC curve

348 (Mukherjee & Singh, 2020) was used to evaluate and compare the results of different

349 models, which takes each value of the predicted results as the possible judgment

350 threshold, and calculates the corresponding sensitivity and specificity accordingly. The

351 false positive rate (1 – specificity) is taken as the horizontal coordinate, and the true

352 positive rate, that is, sensitivity, is drawn as the vertical coordinate. The area under the

353 ROC curve, the AUC value, is a good measure of the model's predictive accuracy, and  
 354 ranging in value from 0.5 to 1; the larger the value, the stronger the judgment of the  
 355 model. In this study, an ROC curve was drawn based on the groundwater nitrate  
 356 concentration and groundwater vulnerability index.

## 357 **4. Results and discussion**

### 358 **4.1 Multi-collinearity diagnosis**

359 The results of the multi-collinearity diagnosis for each evaluation factor are  
 360 presented in Table 2. The tolerance and VIF were 0.35–0.97 and 1.04–2.84, respectively,  
 361 both meeting the conditions of tolerance  $>0.1$  and VIF  $<10$ , which indicates that there  
 362 was no overlap among the nine evaluation factors; thus, the conditions were  
 363 independent and could participate in the model evaluation.

364 **Table 2** Multi-collinearity diagnosis test for all conditioning factors

Factors	Tolerance	VIF
Depth to Water	0.89	1.12
Net Recharge	0.46	2.18
Aquifer Media	0.53	1.87
Soil Media	0.52	1.93
Topography	0.85	1.18
Impact of the Vadose Zone	0.66	1.52
Conductivity of the Aquifer	0.62	1.62
Land use	0.97	1.04
Degree of Groundwater Extraction	0.35	2.84

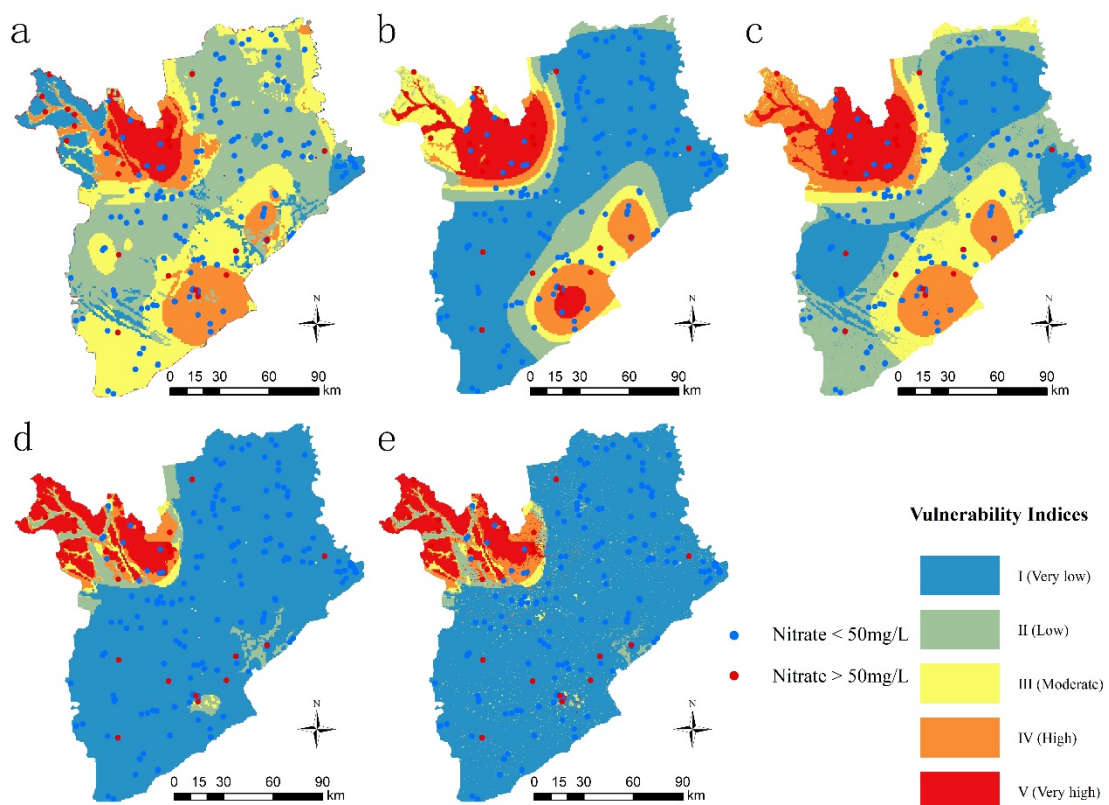
365

### 366 **4.2 Groundwater vulnerability assessment using original DRASTIC** 367 **model**

368 According to the original DRASTIC model, the minimum and maximum values  
 369 of the groundwater vulnerability assessment index in the study area were 94 and 193,

370 respectively. Groundwater vulnerability was classified into five categories based on the  
371 Jenks method in ArcGIS, and a groundwater vulnerability distribution map was drawn  
372 (Fig. 3a).

373 The very low (I) vulnerability region accounted for 9.32% of the study area,  
374 mainly distributed in the hilly area in the northwest. The areas with low (II)  
375 vulnerability were the most distributed, accounting for 41.25% of the study area; the  
376 moderate (III), high (IV), and very high (V) vulnerability regions accounted for 28.97%,  
377 15.12%, and 5.35% of the study area, respectively. Based on this, the overall  
378 groundwater vulnerability in the study area was considered relatively low.



379  
380

381 **Fig. 3** Groundwater vulnerability maps: (a)DRASTIC, (b)AHP-DRASTIC, (c) AHP-

382 DRASTICLE, (d)WOE-DRASTIC, (e) WOE-DRASTICLE.

### 383 **4.3 Groundwater vulnerability assessment using three-scale AHP**

384 To verify the consistency of the judgment matrix, the consistency index values of  
385 the AHP-DRASTIC and AHP-DRASTICLE models were 0.025 and 0.047,  
386 respectively, both of which were <1, indicating that the normalized weight values  
387 passed the consistency test. The weights of the evaluation factors for the two models  
388 are listed in Table 3.

389 **Table 3** Modified weights of the AHP-DRASTIC and AHP-DRASTICLE factors

Factors	Weight	
	AHP-DRASTIC	AHP-DRASTICLE
D (Depth to Groundwater)	0.019	0.010
R (Net Recharge)	0.030	0.023
A (Aquifer Media)	0.152	0.097
S (Soil Media)	0.257	0.244
T (Topography)	0.087	0.060
I (Impact of the Vadose Zone)	0.050	0.037
C (Conductivity of the Aquifer)	0.405	0.359
L(Land use)		0.015
E(Degree of Groundwater Extraction)		0.156

390

391 According to the weights in Table 3, the evaluation factors of the two models were  
392 weighted and superimposed to obtain the distribution map of groundwater vulnerability  
393 in the study area, as shown in Figs. 3b, c. According to the two models, the groundwater  
394 vulnerability in the study area was very low (I) and low (II).

### 395 **4.4 Groundwater vulnerability assessment using WOE**

396 Taking the nitrate concentration as the response factor, there were 254 nitrate  
397 points in the study area. Monitoring wells with  $\text{NO}_3^- \geq 50$  mg/L were selected as the  
398 response factor occurrence point, and there were 26 points with  $\text{NO}_3^- \geq 50$  mg/L. The

399 probability of the occurrence of the response factor was  $P(D) = 0.102$ , and the prior  
400 probability odds were  $O(D) = \frac{P(D)}{1-P(D)} = 0.114$ . The weights calculated according to Eqs. 4  
401 and 5 are shown in Supplementary Table S.

402

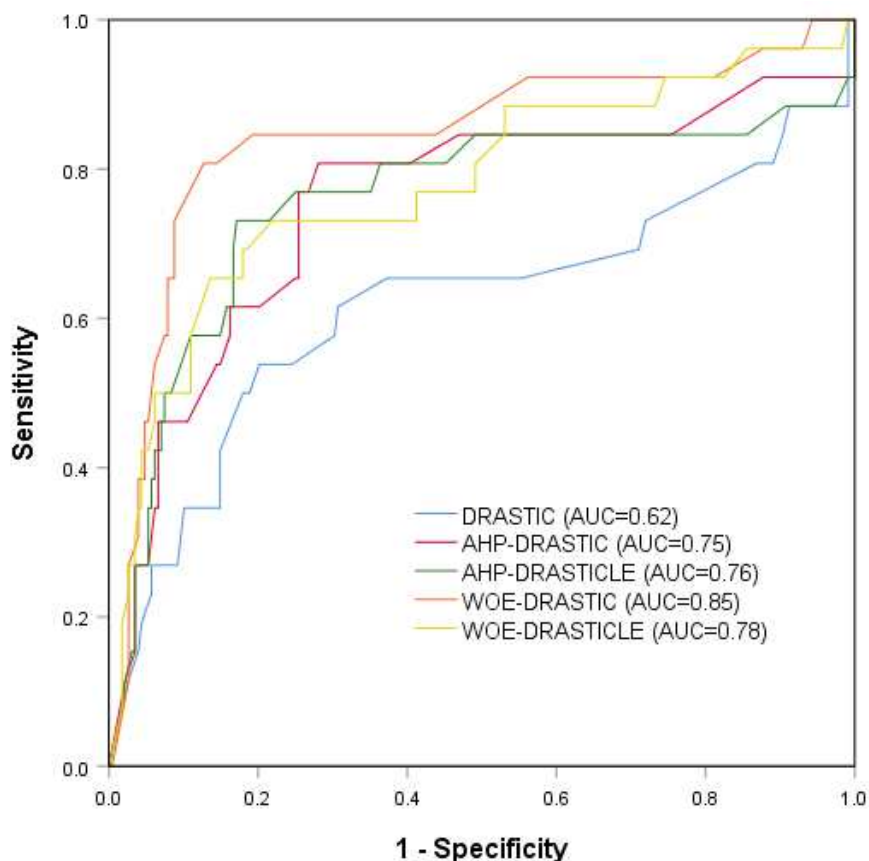
403 According to the weights in Attached Table A, among the factors affecting  
404 groundwater vulnerability, depth to groundwater (D) at 4.6–9.1 m had the highest  
405 impact (1.668) on groundwater vulnerability, net recharge (R) at 177.8–254 mm,  
406 aquifer media (A) at sand and gravel, soil media (S) at loam, topography (T) at 2–6%,  
407 impact of the vadose zone (I) at sand and gravel, conductivity of the aquifer (C) at >81.5  
408 m/d, land use (L) at artificial surface, and degree of groundwater extraction (E) at 50–  
409 70% had the most effect on groundwater pollution probability, respectively.

410 According to Eq. (6), the posterior probabilities of the response factors of the  
411 WOE-DRASTIC and WOE-DRASTICLE models were calculated. The results were  
412 classified into five categories using the Jenks method, as shown in Figs. 3d, e. The  
413 assessment of groundwater vulnerability by WOE showed that the vulnerability of the  
414 WOE-DRASTIC and WOE-DRASTICLE models were mainly very low (I),  
415 accounting for 81.60% and 81.52% of the total area, respectively.

#### 416 **4.5 Evaluation and comparison of model results**

417 As can be seen from Fig. 4, the AUC of the original DRASTIC model is the  
418 minimum (0.62), improved by the three-scale AHP, and the AUCs of AHP-DRASTIC  
419 and AHP-DRASTICLE were 0.75, and 0.76, respectively. The AUC of WOE-

420 DRASTIC was 0.78, and the AUC of WOE-DRASTIC was the largest at 0.845. This  
421 indicates that the results of the two methods (AHP and WOE) were better than those of  
422 the traditional DRASTIC assessment. The three-scale AHP method with the addition of  
423 two evaluation factors yielded better model results, while the result of WOE-DRASTIC  
424 (seven factors) was better than WOE-DRASTIC with nine factors. This is because  
425 the weights calculated for a small number of classes are more robust than those  
426 calculated using a large number of classes, and this is particularly critical when a  
427 relatively small number of points are in the training data(Antonakos & Lambrakis,  
428 2007).



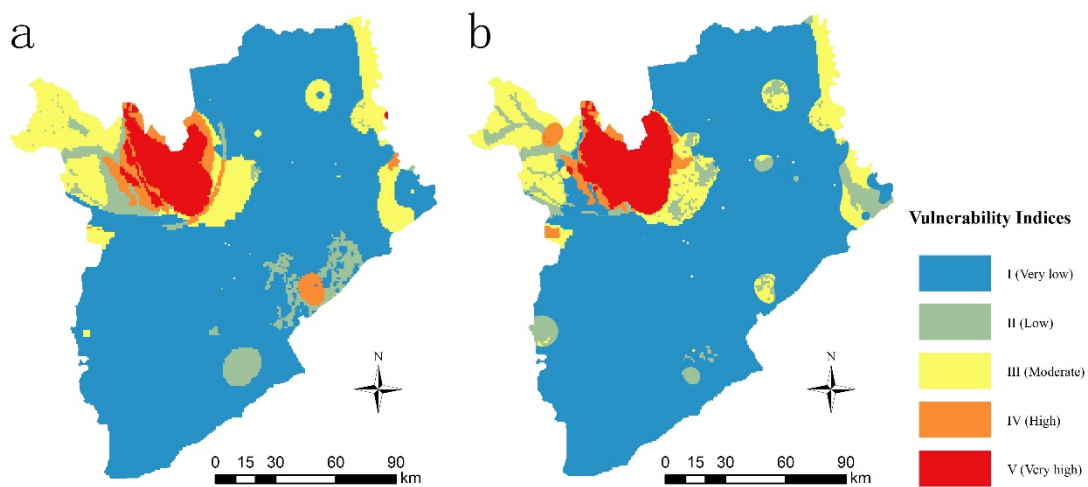
429

430

Fig. 4 ROC curve

431 **4.6 Changes in groundwater vulnerability over time**

432 To study the temporal and spatial pattern change of groundwater vulnerability,  
433 explore its distribution characteristics in different periods, and predict its development  
434 trend, the most effective model, the WOE-DRASTIC model, was selected to evaluate  
435 the groundwater vulnerability in 2000 and 2010. The distribution of groundwater  
436 vulnerability is shown in Fig. 5. In 2000, the very low (I) vulnerability zone accounted  
437 for 72.63%, and the very high (V) vulnerability zone accounted for only 5.14%, mainly  
438 distributed in the Taoer River Fan. In 2010, the areas of very low (I) and very high (V)  
439 groundwater vulnerability accounted for 75.07% and 6.34%, respectively. The very low  
440 (I) vulnerability zone for 81.60% and the very high (V) vulnerability zone for 7.93% in  
441 2018. From 2000 to the present, the proportion of very low vulnerability zones in  
442 groundwater has been gradually increasing, but at the same time the very high  
443 vulnerability zones have also been increasing, with extreme cases. This is related to the  
444 depth of groundwater data.



446 **Fig. 5** Groundwater vulnerability maps: (a) WOE-DRASTIC for 2000, (b) WOE-DRASTIC for

447

2010.

## 448 **4.7 Discussion**

449 The concept of the DRASTIC model is used to evaluate groundwater vulnerability  
450 in the area. The traditional DRASTIC was first used to evaluate the inherent  
451 vulnerability of the aquifer, which is predominantly a low (II) vulnerability (41.25%)  
452 zone, with high (IV) and very high (V) vulnerability zones accounting for 20.47%. As  
453 can be seen from Fig. 3a, 50% of the points with nitrate > 50 mg/L fall into high (IV)  
454 and very high (V) vulnerability zones, and the remaining 50% are mainly distributed in  
455 low (II) vulnerability zones. Finally, 49.6% of nitrate < 50 mg/L points are distributed  
456 in the very low (I) and low (II) vulnerability zones.

457 The seven parameters in the traditional DRASTIC model merely consider the  
458 geological and hydrogeological conditions of the study area and do not consider the  
459 effect of human activities on groundwater. The two added parameters, used to generate  
460 the DRASTICLE model, combined with the three-scale AHP and WOE to modify the  
461 weights of the parameters, found different results as follows. The results of the AHP-  
462 DRASTIC model showed that the very low (I) vulnerability zones had the highest  
463 distribution (55.05%), and the high and very high vulnerability zones showed 19.82%.  
464 A total of 61.5% of the nitrate > 50 mg/L points fell in the high and very high  
465 vulnerability zones and 19% in the very low vulnerability zone. Only 16.2% of the  
466 nitrate < 50 mg/L points fell in the high and very high vulnerability zones and 64% in  
467 the very low vulnerability zone. The evaluation results of AHP-DRASTICLE showed

468 good dispersion, with 73.1% of nitrate >50 mg/L points falling in high and very high  
469 vulnerability zones and 82.5% of nitrate <50 mg/L points falling in moderate, low, and  
470 very low vulnerability zones. After adding the two parameters, the accuracy of the  
471 evaluation results was further improved. While only 38.5% and 57.7% of the nitrate >50  
472 mg/L points for WOE-DRASTIC and WOE-DRASTICLE fell in the high and very high  
473 vulnerability zones, respectively, 94.7% and 77.6% of the nitrate <50 mg/L points fell  
474 in the very low vulnerability zone. These results show that the evaluation results are  
475 more reliable with the addition of two parameters and improved parameter weighting.

476 The WOE results show that depth to groundwater at 4.6–9.1 m had the highest  
477 impact (1.668) on vulnerability, implying that shallower groundwater levels are not  
478 necessarily more vulnerable to pollution. Moreover, with increased net recharge to the  
479 aquifer, the chance of contaminants entering the groundwater becomes greater and the  
480 degree of protection against pollution becomes smaller, with net recharge at 177.8–254  
481 mm having the greatest impact. In general for aquifer media, the larger the medium  
482 particles, the more fissures in the aquifer, and the higher the permeability; thus, the  
483 greater the vulnerability of the aquifer. This was reflected in the model results, which  
484 indicated that sand and gravel had the highest rates. Generally, the type of soil, amount  
485 of expansion and shrinkage, and size of the media particles determine the size of soil  
486 contamination susceptibility. Soils with relatively thick layers, high organic matter  
487 content, and smaller particles have a high capacity to absorb contaminants, as well as  
488 good anti-fouling properties, and low vulnerability. The results of this study show that

489 soil media had great influence on loam, but not gravel. In general regarding topography,  
490 the topographic slope affects the surface runoff volume, runoff velocity, runoff direction,  
491 and residence time. The gentler the slope, the more pollutants leach, and the more likely  
492 they will leach into the groundwater. The results of this study showed that topography  
493 had the greatest effect at 2–6%, not 0–2% as was expected from research by Khosravi  
494 et al. (2018). In general, if the clay gravel content in the vadose zone is higher and the  
495 granules are finer, the permeability of groundwater will be lower. In this study, the WOE  
496 results show that the impact of the vadose zone had the greatest influence on sand and  
497 gravel. Generally, the hydraulic conductivity coefficient of an aquifer reflects the  
498 hydraulic permeability of an aquifer, which determines the migration rate of pollutants  
499 in the aquifer and the difficulty of pollutants entering the groundwater system. In this  
500 study, the results showed that when the conductivity of the aquifer was  $>81.5$  m/d, the  
501 groundwater vulnerability was high. The artificial surface had the greatest influence on  
502 the groundwater vulnerability assessment, likely because the farmers raise livestock  
503 and grow crops and vegetables on their land, thus the associated animal waste,  
504 pesticides, and fertilizers can lead to substantial pollution of groundwater. The degree  
505 of groundwater extraction at 50–70% had the greatest effect on groundwater pollution  
506 probability.

507         The AUC of the ROC curve shows that both the improved AHP-DRASTIC and  
508 WOE-DRASTIC had better evaluation results than the traditional DRASTIC.  
509 Meanwhile, AHP-DRASTICLE was better than AHP-DRASTIC, indicating that the

510 evaluation results are more reliable with the addition of two evaluation factors for the  
511 influence of human activities. The result of WOE-DRASTIC was better than that of  
512 WOE-DRASTICLE because of no enough training points. Findings suggest that both  
513 weight and evaluation factors should be further considered in the improvement of the  
514 model.

## 515 **5. Conclusions**

516 This study evaluates the vulnerability of groundwater in Baicheng City and  
517 optimizes the traditional DRASTIC method to better represent the actual vulnerability  
518 distribution of groundwater. The factors and weights of the DRASTIC method were  
519 improved. In consideration of the influence of human activities on groundwater, two  
520 factors, land use and degree of groundwater extraction, were added to the evaluation  
521 factors. The three-scale AHP and WOE methods were used to improve the weight of  
522 the factors. The results of the five models (DRASTIC, AHP-DRASTIC, AHP-  
523 DRASTICLE, WOE-DRASTIC, WOE-DRASTICLE) were compared using the ROC  
524 curve. Results showed that the model improvements proposed in this study had obvious  
525 effects: the model evaluation results were more accurate and had a higher correlation  
526 with nitrate concentration. Moreover, the evaluation results were shown to have  
527 improved accuracy after adding two factors to the AHP method. For the WOE method,  
528 the AUC of WOE-DRASTICLE was smaller than that of WOE-DRASTIC, which is to  
529 in the case of the few training points, the fewer evaluation factors, hence the evaluation  
530 results had higher accuracy. In the future research, if more training points exist, it can

531 be considered to add more evaluation factors into the WOE method.

532 The WOE-DRASTIC model was selected to evaluate the groundwater  
533 vulnerability of Baicheng City in 2000 and 2010 and found that the groundwater  
534 vulnerability in this region was mainly very low and low. From 2000 to 2018, the  
535 proportion of low groundwater vulnerability also increased gradually from 72.63% to  
536 81.60%. The high vulnerability was distributed in the Taoer River fan in the northwest  
537 of the study area. Importantly, it should be noted that groundwater pollution may still  
538 occur in very low or low vulnerability areas, though compared with areas of high  
539 vulnerability, these areas are less vulnerable to human activities and natural  
540 environmental pollution. Overall, it is recommended that government departments  
541 should facilitate reasonable control of groundwater pollution prevention and extraction  
542 according to changes in groundwater vulnerability in the region. This study therefore  
543 provides a theoretical basis for the Baicheng municipal government to manage and  
544 exploit groundwater resources.

545

## 546 **Supplementary Material**

547 **Table S** Spatial correlation between nitrate and factors using WOE model

Factors	Range	Class	No.of pixels	Percentage of domain(%)	No.of nitrate	Percentage of nitrate(%)	W+	W-	Sc	C	C/Sc
D	15.2-22.9	3	19525	0.07	0	0.00	None	0.001	None	None	None
	9.1-15.2	5	1477578	5.16	1	3.85	-0.294	0.014	1.020	-0.308	-0.302
	4.6-9.1	7	20997450	73.36	23	88.46	0.187	-0.837	0.614	1.024	1.668
	1.5-4.6	9	6116909	21.37	2	7.69	-1.022	0.160	0.736	-1.182	-1.606
	0-1.5	10	12045	0.04	0	0.00	None	0.000	None	None	None
R	50.8-101.6	3	31404	88.35	21	80.77	-0.090	0.501	0.498	-0.591	-1.187
	101.6-177.8	6	278	0.78	0	0.00	None	0.008	None	None	None
	177.8-254	8	3862	10.87	5	19.23	0.571	-0.099	0.498	0.669	1.345
A	Metamorphic/Igneous	3	1706500	5.96	3	11.54	0.661	-0.061	0.614	0.722	1.176
	Massive Sandstone	6	25564772	89.28	17	65.38	-0.311	1.172	0.412	-1.483	-3.598
	Sand and Gravel	8	1364024	4.76	6	23.08	1.578	-0.214	0.465	1.791	3.849
S	Loam	5	2099007	7.34	6	23.08	1.146	-0.186	0.465	1.332	2.861
	Sand	9	23941055	83.71	20	76.92	-0.085	0.348	0.465	-0.433	-0.930
	Gravel	10	2559880	8.95	0	0.00	None	0.094	None	None	None
T	>18	1	2090	0.01	0	0.00	None	0.000	None	None	None
	12-18	3	10724	0.04	0	0.00	None	0.000	None	None	None
	6-12	5	94208	0.33	0	0.00	None	0.003	None	None	None
	2-6	9	1046784	3.66	1	3.85	0.050	-0.002	1.020	0.052	0.051
	0-2	10	27451069	95.97	25	96.15	0.002	-0.048	1.020	0.050	0.049
I	Silt/Clay	1	2738401	9.61	5	19.23	0.694	-0.113	0.498	0.806	1.620
	limit loam	5	7216826	25.33	3	11.54	-0.786	0.169	0.614	-0.956	-1.557
	Sandstone	6	17277701	60.63	13	50.00	-0.193	0.239	0.392	-0.432	-1.101
	Sand and Gravel	8	1263549	4.43	5	19.23	1.467	-0.168	0.498	1.635	3.287

C	0-4.1	1	7210489	25.19	2	7.69	-1.186	0.210	0.736	-1.396	-1.897
	4.1-12.2	2	8382437	29.29	3	11.54	-0.931	0.224	0.614	-1.155	-1.882
	12.2-28.5	4	3721649	13.00	1	3.85	-1.218	0.100	1.020	-1.318	-1.292
	28.5-40.7	6	1931868	6.75	1	3.85	-0.562	0.031	1.020	-0.593	-0.581
	40.7-81.5	8	2781926	9.72	3	11.54	0.172	-0.020	0.614	0.192	0.313
	>81.5	10	4595235	16.05	16	61.54	1.344	-0.781	0.403	2.124	5.270
	L	Forest	1	88719	0.31	0	0.00	None	0.003	None	None
natural grass		2	5762547	20.13	3	11.54	-0.556	0.102	0.614	-0.659	-1.073
Wetland		3	321146	1.12	0	0.00	None	0.011	None	None	None
Water Bodies		5	848979	2.97	0	0.00	None	0.030	None	None	None
Cultivated Land		6	17314166	60.48	6	23.08	-0.963	0.666	0.465	-1.629	-3.501
Bareland		7	3401822	11.88	0	0.00	None	0.127	None	None	None
Artificial Surface		10	891087	3.11	17	65.38	3.045	-1.029	0.412	4.074	9.883
E	0-20%	1	1127	3.17	0	0.00	None	0.032	None	None	None
	20%-50%	3	25153	70.77	11	42.31	-0.514	0.680	0.397	-1.194	-3.007
	50%-70%	6	6198	17.44	10	38.46	0.791	-0.294	0.403	1.085	2.690
	80%-100%	9	3066	8.63	5	19.23	0.802	-0.123	0.498	0.925	1.858

## 549 **Acknowledgment**

550 This study was supported by the National Natural Science Foundation of China,  
551 Research on the Impact of In-situ Oil Shale Exploitation on Groundwater Environment  
552 [project number 41572216], the China Geological Survey project, regional water  
553 resources survey methods, and groundwater ecological threshold survey research  
554 [project number DD20190340], Geological Exploration Fund of Jilin Province,  
555 Geothermal Resources Survey in the Middle and West of Jilin Province [project number  
556 2018-13]; Special Project of the Provincial University Co-Construction Program-  
557 Frontier Science and Technology Guidance Category, Research on the Interdependent  
558 Ecosystem and Sustainable Utilization of Natural Mineral Water in Changbai Mountain  
559 [project number SXGJQY2017-6]; Key research and development program of Shaanxi  
560 Province, Construction of Big Data Platform for Geotechnical Engineering [project  
561 number 2017ZDCXL-SF-03-01-01]. The authors would like to thank Jilin Jingyu field  
562 scientific observation and research base of volcanoes and mineral springs, which  
563 provided the necessary data to conduct this study. We thank the anonymous reviewers  
564 and editors who contributed valuable comments, which were useful in improving the  
565 quality of the manuscript.

566 **Author contribution:** Mingjun Liu: Writing - original draft, Data curation, Formal  
567 analysis. Changlai Xiao: Conceptualization, Writing -review, Supervision, Funding  
568 acquisition. Xiujuan Liang: Methodology & editing, Formal analysis.

569 **Data availability** The dataset used and/or analyzed during the current study are

570 available from the corresponding author on reasonable request.

571 **Compliance with ethical standards**

572 **Ethics approval and consent to participate** Not applicable.

573 **Consent for publication** Not applicable.

574 **Declaration of competing interest**

575 The authors declare that they have no known competing financial interests or  
576 personal relationships that could have appeared to influence the work reported in this  
577 paper.

578

579

580 **References**

581 Abu-Bakr, H. A. e.-A. (2020). Groundwater vulnerability assessment in different types  
582 of aquifers. *Agricultural Water Management*, 240.

583 doi:10.1016/j.agwat.2020.106275

584 Agterberg, & F., P. (1989). Computer programs for mineral exploration. *Science*,  
585 245(4913), 76-81. doi:10.1126/science.245.4913.76

586 Al-Adamat, R. A. N., Foster, I. D. L., & Baban, S. M. J. (2003). Groundwater  
587 vulnerability and risk mapping for the Basaltic aquifer of the Azraq basin of Jordan  
588 using GIS, Remote sensing and DRASTIC. *Applied Geography*, 23(4), 303-324.

589 doi:10.1016/j.apgeog.2003.08.007

590 Aller, L., Bennett, T., Lehr, J., Petty, R., & Hackett, G. (1987). DRASTIC: Standardized

591 system for evaluating groundwater pollution potential using hydrogeologic settings.  
592 *Journal of the Geological Society of India*, 29.

593 Almasri, M. N. (2008). Assessment of intrinsic vulnerability to contamination for Gaza  
594 coastal aquifer, Palestine. *J Environ Manage*, 88(4), 577-593.  
595 doi:10.1016/j.jenvman.2007.01.022

596 An, Y., & Lu, W. (2018). Assessment of groundwater quality and groundwater  
597 vulnerability in the northern Ordos Cretaceous Basin, China. *Arabian Journal of*  
598 *Geosciences*, 11(6). doi:10.1007/s12517-018-3449-y

599 Antonakos, A. K., & Lambrakis, N. J. (2007). Development and testing of three hybrid  
600 methods for the assessment of aquifer vulnerability to nitrates, based on the drastic  
601 model, an example from NE Korinthia, Greece. *Journal of Hydrology*, 333(2-4),  
602 288-304. doi:10.1016/j.jhydrol.2006.08.014

603 Arabameri, A., Rezaei, K., Cerda, A., Lombardo, L., & Rodrigo-Comino, J. (2019).  
604 GIS-based groundwater potential mapping in Shahroud plain, Iran. A comparison  
605 among statistical (bivariate and multivariate), data mining and MCDM approaches.  
606 *Science Of the Total Environment*, 658, 160-177.  
607 doi:10.1016/j.scitotenv.2018.12.115

608 Babiker, I. S., Mohamed, M. A., Hiyama, T., & Kato, K. (2005). A GIS-based  
609 DRASTIC model for assessing aquifer vulnerability in Kakamigahara Heights, Gifu  
610 Prefecture, central Japan. *Sci Total Environ*, 345(1-3), 127-140.  
611 doi:10.1016/j.scitotenv.2004.11.005

612 Bai, L., Wang, Y., & Meng, F. (2012). Application of DRASTIC and extension theory  
613 in the groundwater vulnerability evaluation. *Water and Environment Journal*, 26(3),  
614 381-391. doi:10.1111/j.1747-6593.2011.00298.x

615 Barber, Bates, C., Barron, L., & Allison, R. (1998). Comparison of standardised and  
616 region-specific methods for assessment of the vulnerability of groundwater to  
617 pollution; a case study in an agricultural catchment.

618 Barzegar, R., Moghaddam, A. A., & Baghban, H. (2015). A supervised committee  
619 machine artificial intelligent for improving DRASTIC method to assess  
620 groundwater contamination risk: a case study from Tabriz plain aquifer, Iran.  
621 *Stochastic Environmental Research and Risk Assessment*, 30(3), 883-899.  
622 doi:10.1007/s00477-015-1088-3

623 Barzegar, R., Moghaddam, A. A., Deo, R., Fijani, E., & Tziritis, E. (2018). Mapping  
624 groundwater contamination risk of multiple aquifers using multi-model ensemble  
625 of machine learning algorithms. *Sci Total Environ*, 621, 697-712.  
626 doi:10.1016/j.scitotenv.2017.11.185

627 Bojórquez-Tapia, L. A., Cruz-Bello, G. M., Luna-González, L., Juárez, L., & Ortiz-  
628 Pérez, M. A. (2009). V-DRASTIC: Using visualization to engage policymakers in  
629 groundwater vulnerability assessment. *Journal of Hydrology*, 373(1-2), 242-255.  
630 doi:10.1016/j.jhydrol.2009.05.005

631 Bonfanti, M., Ducci, D., Masetti, M., Sellerino, M., & Stevenazzi, S. (2016). Using  
632 statistical analyses for improving rating methods for groundwater vulnerability in

633 contamination maps. *Environmental Earth Sciences*, 75(12). doi:ARTN  
634 100310.1007/s12665-016-5793-0

635 Brindha, K., & Elango, L. (2015). Cross comparison of five popular groundwater  
636 pollution vulnerability index approaches. *Journal of Hydrology*, 524, 597-613.  
637 doi:10.1016/j.jhydrol.2015.03.003

638 Feng, X. (2019). *Study on the Protection Scheme of Groundwater Resources in*  
639 *Baicheng City* (master), Jilin University, Available from Cnki

640 Ferreira, J. P. L., & Oliveira, M. M. (2004). Groundwater vulnerability assessment in  
641 Portugal. *Geofísica Internacional*, 43(4), 541-550.

642 Ghazavi, R., & Ebrahimi, Z. (2015). Assessing groundwater vulnerability to  
643 contamination in an arid environment using DRASTIC and GOD models.  
644 *International Journal of Environmental Science and Technology*, 12(9), 2909-2918.  
645 doi:10.1007/s13762-015-0813-2

646 Gogu, R. C., & Dassargues, A. (2000). Current trends and future challenges in  
647 groundwater vulnerability assessment using overlay and index methods.  
648 *Environmental Geology*, 39(6), 549-559. doi:DOI 10.1007/s002540050466

649 Huan, H., Wang, J., & Teng, Y. (2012). Assessment and validation of groundwater  
650 vulnerability to nitrate based on a modified DRASTIC model: a case study in Jilin  
651 City of northeast China. *Sci Total Environ*, 440, 14-23.  
652 doi:10.1016/j.scitotenv.2012.08.037

653 Huan, H., Wang, J. S., Zhai, Y. Z., Xi, B. D., Li, J., & Li, M. X. (2016). Quantitative

654 evaluation of specific vulnerability to nitrate for groundwater resource protection  
655 based on process-based simulation model. *Science Of the Total Environment*, 550,  
656 768-784. doi:10.1016/j.scitotenv.2016.01.144

657 Jhariya, D. C. (2019). Assessment of Groundwater Pollution Vulnerability Using GIS-  
658 Based DRASTIC Model and its Validation Using Nitrate Concentration in Tandula  
659 Watershed, Chhattisgarh. *Journal of the Geological Society of India*, 93(5), 567-  
660 573. doi:10.1007/s12594-019-1218-5

661 Kazakis, N., & Voudouris, K. S. (2015). Groundwater vulnerability and pollution risk  
662 assessment of porous aquifers to nitrate: Modifying the DRASTIC method using  
663 quantitative parameters. *Journal of Hydrology*, 525, 13-25.  
664 doi:10.1016/j.jhydrol.2015.03.035

665 Khan, R., & Jhariya, D. C. (2019). Assessment of Groundwater Pollution Vulnerability  
666 Using GIS Based Modified DRASTIC Model in Raipur City, Chhattisgarh. *Journal*  
667 *of the Geological Society of India*, 93(3), 293-304. doi:10.1007/s12594-019-1177-  
668 x

669 Khosravi, K., Sartaj, M., Tsai, F. T., Singh, V. P., Kazakis, N., Melesse, A. M., Prakash,  
670 I., Tien Bui, D., & Pham, B. T. (2018). A comparison study of DRASTIC methods  
671 with various objective methods for groundwater vulnerability assessment. *Sci Total*  
672 *Environ*, 642, 1032-1049. doi:10.1016/j.scitotenv.2018.06.130

673 Mukherjee, I., & Singh, U. K. (2020). Delineation of groundwater potential zones in a  
674 drought-prone semi-arid region of east India using GIS and analytical hierarchical

675 process techniques. *Catena*, 194. doi:ARTN 10468110.1016/j.catena.2020.104681

676 O'Brien, R. M. (2007). A caution regarding rules of thumb for variance inflation factors.

677 *Quality & Quantity*, 41(5), 673-690. doi:10.1007/s11135-006-9018-6

678 Omotola, O. O., Oladapo, M. I., & Akintorinwa, O. J. (2020). Modeling assessment of

679 groundwater vulnerability to contamination risk in a typical basement terrain case

680 of vulnerability techniques application comparison study. *Modeling Earth Systems*

681 *and Environment*, 6(3), 1253-1280. doi:10.1007/s40808-020-00720-1

682 Pacheco, F. A., Pires, L. M., Santos, R. M., & Sanches Fernandes, L. F. (2015). Factor

683 weighting in DRASTIC modeling. *Sci Total Environ*, 505, 474-486.

684 doi:10.1016/j.scitotenv.2014.09.092

685 Perrin, J., Cartannaz, C., Noury, G., & Vanoudheusden, E. (2015). A multicriteria

686 approach to karst subsidence hazard mapping supported by weights-of-evidence

687 analysis. *Engineering Geology*, 197, 296-305. doi:10.1016/j.enggeo.2015.09.001

688 Rezaei, F., Safavi, H. R., & Ahmadi, A. (2013). Groundwater Vulnerability Assessment

689 Using Fuzzy Logic: A Case Study in the Zayandehrood Aquifers, Iran.

690 *Environmental Management*, 51(1), 267-277. doi:10.1007/s00267-012-9960-0

691 Saaty, T., & Kearns, K. (1985). The Analytic Hierarchy Process. *analytical planning*,

692 19-62. doi:10.1016/B978-0-08-032599-6.50008-8

693 Sahoo, M., Sahoo, S., Dhar, A., & Pradhan, B. (2016). Effectiveness evaluation of

694 objective and subjective weighting methods for aquifer vulnerability assessment in

695 urban context. *Journal of Hydrology*, 541, 1303-1315.

696 doi:10.1016/j.jhydrol.2016.08.035

697 Sener, E., & Davraz, A. (2012). Assessment of groundwater vulnerability based on a  
698 modified DRASTIC model, GIS and an analytic hierarchy process (AHP) method:  
699 the case of Egirdir Lake basin (Isparta, Turkey). *Hydrogeology Journal*, 21(3), 701-  
700 714. doi:10.1007/s10040-012-0947-y

701 Shrestha, S., Semkuyu, D. J., & Pandey, V. P. (2016). Assessment of groundwater  
702 vulnerability and risk to pollution in Kathmandu Valley, Nepal. *Sci Total Environ*,  
703 556, 23-35. doi:10.1016/j.scitotenv.2016.03.021

704 Thirumalaivasan, D., Karmegam, M., & Venugopal, K. (2003). AHP-DRASTIC:  
705 software for specific aquifer vulnerability assessment using DRASTIC model and  
706 GIS. *Environmental Modelling & Software*, 18(7), 645-656. doi:10.1016/s1364-  
707 8152(03)00051-3

708 Victorine Neh, A., Ako Ako, A., Richard Ayuk, A., & Hosono, T. (2015). DRASTIC-  
709 GIS model for assessing vulnerability to pollution of the phreatic aquiferous  
710 formations in Douala–Cameroon. *Journal of African Earth Sciences*, 102, 180-190.  
711 doi:10.1016/j.jafrearsci.2014.11.001

712 Voutchkova, D. D., Schullehner, J., Rasmussen, P., & Hansen, B. (2021). A high-  
713 resolution nitrate vulnerability assessment of sandy aquifers (DRASTIC-N). *J*  
714 *Environ Manage*, 277, 111330. doi:10.1016/j.jenvman.2020.111330

715 Wang, J. L., & Yang, Y. S. (2008). An approach to catchment-scale groundwater nitrate  
716 risk assessment from diffuse agricultural sources: a case study in the Upper Bann,

717 Northern Ireland. *Hydrological Processes*, 22(21), 4274-4286.  
718 doi:10.1002/hyp.7036

719 Wu, X., Li, B., & Ma, C. (2018). Assessment of groundwater vulnerability by applying  
720 the modified DRASTIC model in Beihai City, China. *Environ Sci Pollut Res Int*,  
721 25(13), 12713-12727. doi:10.1007/s11356-018-1449-9

722 Zhang, Z. J., Zuo, R. G., & Xiong, Y. H. (2016). A comparative study of fuzzy weights  
723 of evidence and random forests for mapping mineral prospectivity for skarn-type  
724 Fe deposits in the southwestern Fujian metallogenic belt, China. *Science China-  
725 Earth Sciences*, 59(3), 556-572. doi:10.1007/s11430-015-5178-3

726 Zuo, J. (1988). The indirect method of judgment matrix in analytic hierarchy process.  
727 *Systems engineering*(06), 56-63. doi:CNKI:SUN:GCXT.0.1988-06-013  
728